EUROPEAN ORGANIZATION FOR NUCLEAR RESEARCH

A STUDY OF THE CHARGE-EXCHANGE REACTION $pp \to n\Delta^{++}(1232)$ AT ISR ENERGIES

H. de Kerret, E. Nagy[1], R.S. Orr, M. Regler[2],
W. Schmidt-Parzefall and K. Winter

CERN, Geneva, Switzerland

A. Brandt, H. Dibon[2], G. Flügge[3],
F. Niebergall and P.E. Schumacher

II. Institut für Experimentalphysik, Hamburg, Germany

K.R. Schubert

Institut für Hochenergiephysik, Universität Heidelberg, Germany

J.J. Aubert, C. Broll, G. Coignet, J. Favier,
L. Massonnet and M. Vivargent

Laboratoire d'Annecy de Physique des Particules, Annecy, France

W. Bartl, H. Eichinger, Ch. Gottfried and G. Neuhofer

Institut für Hochenergiephysik, Vienna, Austria

ABSTRACT

We report on a study of the charge-exchange reaction $pp \to n\Delta^{++}(1232)$ at the CERN Intersecting Storage Rings (ISR) in the energy range $\sqrt{s}$ = 23 to 53 GeV. From our analysis of the energy dependence of the total cross-section, of the differential cross-section $d\sigma/dt$ and of the decay angular distributions we find evidence that pion exchange is dominant up to $\sqrt{s}$ = 23 GeV and that $(\rho + A_2)$ exchange dominates the reaction for $\sqrt{s} \geq 30$ GeV, as described by simple Regge-pole models.

Geneva - 24 June 1977

(Submitted to Physics Letters B)

---

1) Visitor from the Central Research Institute for Physics, Budapest, Hungary.
2) Now at Institut für Hochenergiephysik, Vienna, Austria.
3) Now at DESY, Hamburg, Germany.

The study of charge-exchange reactions has been of outstanding importance because of their simplicity for our theoretical understanding of strong interactions. In the case of proton charge exchange these are the reactions:

$$pn \to np \tag{1}$$

and

$$pp \to n\Delta^{++}(1232) . \tag{2}$$

At low energies [1] (p_{lab} < 50 GeV/c) their total cross-sections were found to decrease approximately like p_{lab}^{-2}. These reactions are fairly well described [2] in terms of exchange of a single Regge pole, that of the pion. It is expected that, at sufficiently high energy, the amplitudes of higher lying poles such as the ρ and the A_2, would start to dominate, manifesting themselves by a less rapid energy dependence of their cross-section, in the form p_{lab}^{-1}.

Our initial study [3] of reaction (2) at the CERN ISR had not given conclusive results because of lack of statistics. We are reporting here new results on a study of reaction (2) at centre-of-mass energies $\sqrt{s}$ = 23, 31, 45, and 53 GeV using the Split Field Magnet (SFM) at the CERN Intersecting Storage Rings (ISR).

The SFM detector has been described elsewhere [4]; it consists of two forward telescopes equipped with 28 multiwire proportional chambers, of two wire planes each, and of a central detector [5] equipped with six multiplane proportional chambers. The average magnetic field is 0.5 T at $\sqrt{s}$ = 23 GeV, 0.65 T at $\sqrt{s}$ = 30 GeV, and 1 T at $\sqrt{s}$ = 45 and 53 GeV, resulting in a mass resolution of 20 MeV (FWHM) for $\Delta^{++}(1232)$. We have added two neutron hodoscopes [6] to the forward telescopes, consisting of a carbon converter plate (40 × 40 cm^2) of 10 cm thickness and multiwire proportional chambers to reconstruct the neutron interaction point. The neutron hodoscopes are positioned at 9 m distance from the beams intersection; they detect neutrons within the angular range from 0 to 23 mrad with an efficiency of 6% and a resolution of ±2.5 mm on the neutron vertex.

Events are selected in three steps; a fast trigger requires at least one charged particle in one of the telescopes, using signals from the proportional wire chambers, a neutron conversion in the opposite hemisphere and no charged particle in the central detector. A slow trigger selects events using memory levels of groups of wires [7] with a decision time of 2 μsec. It requires two charged particles in one telescope and no charged particle in the opposite, neutron-side, telescope. Events with single-prong showers in the neutron detector were rejected on-line by a fast filter code.

The geometrical acceptance of the neutron hodoscopes extends from $t = 0$ to $-t = 0.1$, 0.15, 0.32, and 0.5 GeV at $\sqrt{s} = 23$, 31, 45, and 53 GeV, respectively.

We have processed events with an off-line analysis chain consisting of three programs. A pattern recognition program [8] finds track candidates and the neutron interaction point. The trajectories of the charged particles are reconstructed using a geometrical fit program [9], and their direction, charge, momentum, and vertex are calculated. Finally, a kinematical fit with three constraints is performed assuming that the positive particle of higher momentum is the proton and the other one is the pion of reaction (2). This choice is always correct for $(p\pi^+)$ mass values below 1350 MeV.

In order to separate genuine events of reaction (2) from the large background, we have examined the distribution of missing momentum calculated by imposing energy and momentum conservation. We select events satisfying the following criteria:

i) invariant mass $M(p\pi^+) < 1350$ MeV/c^2;

ii) missing transverse momentum in the plane of magnetic deflection: $|\Delta p_x| < 100$ MeV/c;

iii) missing longitudinal neutron momentum $|\Delta p_n| < 3$ GeV/c;

and obtain a distribution of events in the other component of missing transverse momentum, Δp_z, perpendicular to the plane of magnetic deflection, as shown in Fig. 1a for $\sqrt{s} = 23$ GeV. We observe an accumulation of events around $\Delta p_z = 0$ which we attribute to reaction (2) and a broad distribution due to background. The mass distribution of events with $|\Delta p_z| < 50$ MeV/c, displayed in Fig. 1b, shows clear evidence of the $\Delta^{++}(1232)$. To subtract the background in this interval, we use the $|\Delta p_z|$ distribution of a sample of background events chosen by the condition $200 < |\Delta p_x| < 300$ MeV/c and normalized to the background region with $|\Delta p_z| > 200$ MeV/c. This agrees well with a simple linear extrapolation of this region to the $|\Delta p_z| < 50$ MeV/c bin.

To correct the differential distributions, we use the corresponding normalized distributions of background events chosen by the criterion:

$$200 < |\Delta p_x| < 300 \text{ MeV/c}$$
$$100 < |\Delta p_z| < 200 \text{ MeV/c} .$$

The number of events of reaction (2) and of the background found in this way is summarized in Table 1.

The observed number of events and their differential distributions must be corrected for the geometrical acceptance of the detector and of the trigger and selection criteria, for the neutron detection efficiency, for loss of events due to absorption and scattering in the beam tube and in the frames of the wire chambers. Events were simulated by Monte Carlo methods using the following initial parametrization of the fourfold differential cross-section of reaction (2):

i) dependence on four-momentum transfer t as exp (12t);

ii) a Breit-Wigner mass distribution of the Δ^{++} around M = 1228 MeV/c^2 with a width Γ = 60 MeV/c^2;

iii) a decay angular distribution in the Jackson [10] frame, following low-energy data [1].

These events are processed in the same way as the observed ones, their distributions are compared, and the parametrization of the t distribution and of the decay angular distribution is corrected at each energy. After a second iteration the data are described in a satisfactory way.

Integrating over the differential distributions and assuming an exponential dependence in extrapolating $d\sigma/dt$ to large values of t we find the total cross-section. The absolute normalization is obtained as described before [3] using the Van der Meer method [11]. The results are summarized in Table 1 and shown in Fig. 2 together with data at lower energies in the form of $p_{lab}^2 \cdot \sigma_T$ as a function of equivalent beam momentum p_{lab}.

Below $p_{lab} \simeq 500$ GeV/c we observe consistency with a p_{lab}^2 dependence, suggesting dominance of one-pion exchange. A dramatic change takes place at $p_{lab} \simeq 500$ GeV/c. Above this momentum the cross-section is consistent with a p_{lab}^{-1} dependence, suggesting dominance of ρ and A_2 exchange.

The energy dependence of the differential cross-section $d\sigma/dt$, shown in Fig. 3, is consistent with this picture. At $\sqrt{s} = 23$ GeV we observe an exponential dependence starting at t = 0, typical of one-pion exchange [1]. At higher energies we observe a flat t dependence near t = 0, consistent with the typical picture of a helicity-flip amplitude in ρ exchange; for comparison we also show the t dependence of the reaction

$$\pi^- p \rightarrow \pi^0 n \tag{3}$$

as observed at $p_{lab} = 199.3$ GeV/c [12], which is well described by ρ exchange.

We observe a third, but weaker, piece of evidence in the energy dependence of the spin density matrix elements. The decay angular distribution of a spin $3/2$ state is described by the expression:

$$W_{3/2}\left(\theta_J,\phi_J\right) \propto \rho_{33} \sin^2 \theta_J + (0.5 - \rho_{33}) \left(\frac{1}{3} + \cos^2 \theta_J\right)$$
$$- \left(\frac{2}{\sqrt{3}}\right) \left(\mathrm{Re}\, \rho_{3,-1} \sin^2 \theta_J \cos 2\phi_J + \mathrm{Re}\, \rho_{3,1} \sin 2\theta_J \cos \phi_J\right) . \tag{4}$$

The fit of expression (4) to our events integrated over the range $0 < |t| < 0.3$ GeV^2, results in a determination of a set of ρ_{ij} values presented in Table 2 with the corresponding fit qualities. The value of ρ_{33} increases with $\sqrt{s}$, reflecting an increase of $d\sigma/d \cos \theta_J$ at $\theta_J = 90°$ as expected for ρ exchange [13].

In conclusion, we have found clear experimental evidence for a long-ago predicted claim of Regge theory, the dominance of higher lying poles at high energy.

We wish to thank C. Meyers for the very useful discussions we have had with him, and N. Kwak for contributions in the early stages of the experiment. The excellent support of the SFM detector and data-handling groups is gratefully acknowledged. The group from the University of Hamburg wishes to acknowledge financial support from the Bundesministerium für Forschung und Technologie, Bonn, Germany.

Table 1

Total cross-sections

$\sqrt{s}$ (GeV)	p_{lab} (GeV/c)	Number of events after background subtraction	Background (%)	σ_{tot} (μb)
23	280	240	24	1.2 ± 0.17
31	510	110	22	0.58 ± 0.09
45	1090	126	31	0.21 ± 0.04
53	1500	58	37	0.17 ± 0.04

Table 2

Spin density matrix elements

$\sqrt{s}$ (GeV)	ρ_{33}	Re $\rho_{3,-1}$	Re $\rho_{3,1}$	χ^2 confidence level (%)
23	0.24 ± 0.07	0.14 ± 0.05	0.06 ± 0.05	34
31	0.31 ± 0.1	0.069 ± 0.05	-0.2 ± 0.1	75
45	0.44 ± 0.11	0.11 ± 0.08	-0.11 ± 0.1	75

REFERENCES

[1] E. Bracci, J.P. Droulez, E. Flaminio, J.P. Hansen and D.R.O. Morrison, CERN/HERA 73-1. References to earlier work may be found therein and in J.D. Mountz, G.A. Smith, A.J. Lennox, J.A. Poirier, P.J. Prukop, C.A. Rey, O.R. Sander, P. Kirk, R.D. Klemm and I. Spirn, Phys. Rev. D12 (1975) 1211.

[2] Zming Ma, G.A. Smith, R.J. Sprafka and G.T. Williamson, Phys. Rev. Letters 24 (1970) 1031.

[3] N. Kwak, E. Nagy, M. Regler, W. Schmidt-Parzefall, K.R. Schubert, K. Winter, A. Brandt, H. Dibon, G. Flügge, F. Niebergall, P.E. Schumacher, J.J. Aubert, C. Broll, G. Coignet, J. Favier, L. Massonnet, M. Vivargent, W. Bartl, H. Eichinger, Ch. Gottfried and G. Neuhofer, Phys. Letters 62B (1976) 359.

[4] R. Bouclier, G. Charpak, E. Chesi, L. Dumps, H.G. Fischer, H.J. Hilke, P.G. Innocenti, G. Maurin, A. Minten, L. Naumann, F. Piuz, J.C. Santiard and O. Ullaland, Nuclear Instrum. Methods 115 (1974) 235.

[5] R. Bouclier, R.C.A. Brown, E. Chesi, L. Dumps, H.G. Fischer, P.G. Innocenti, G. Maurin, A. Minten, L. Naumann, F. Piuz and O. Ullaland, Nuclear Instrum. Methods 125 (1975) 19.

[6] J.J. Aubert, C. Broll, G. Coignet, J. Favier, L. Massonnet, D.B. Smith, M. Vivargent and H. Dibon, Proc. Internat. Conf. on Instrumentation for High-Energy Physics, Frascati, 1973 (CNEN, Frascati, 1973), p. 410.

[7] A. Brandt, H. Dibon, G. Flügge, F. Niebergall, K.R. Schubert, P.E. Schumacher and W. Wilmsen, Nuclear Instrum. Methods 126 (1975) 519.

[8] H. Grote, M. Metcalf, C. Onions and F. Ranjard, CERN SFM Users' Guide, OM Div. Note AP/18-CERN (1975).

[9] M. Metcalf, M. Regler and C. Broll, CERN 73-2 (1973).

[10] K. Gottfried and J.D. Jackson, Nuovo Cimento 33 (1964) 309.

[11] S. Van der Meer, CERN Internal Report ISR-PO/68-31.

[12] A.V. Barnes, D.J. Mellema, A.V. Tollestrup, R.L. Walker, O.I. Dahl, R.A. Johnson, R.W. Kenney and M. Pripstein, Phys. Rev. Letters 37 (1976) 76.

[13] L. Stodolsky and J.J. Sakurai, Phys. Rev. Letters 11 (1963) 90.
M. Krammer and V. Maor, Nuovo Cimento 52A (1967) 308.

Figure captions

Fig. 1 : a) Distribution in one transverse component of missing momentum $|\Delta p_z|$, observed at $\sqrt{s}$ = 23 GeV. Events in the shaded area are selected. The dashed histogram represents the estimate of background. The full line shows a linear background extrapolation.

b) Invariant mass of $(p\pi^+)$, at $\sqrt{s}$ = 23 GeV, of events with small missing transverse momentum $|\Delta p_z| < 50$ MeV/c. The dashed line represents simulated events generated following a Breit-Wigner parametrization of the $\Delta^{++}(1232)$.

Fig. 2 : Total cross-section of the reaction $pp \to n\Delta^{++}(1232)$ multiplied by the square of the equivalent laboratory momentum as a function of p_{lab}.

Fig. 3 : Differential cross-sections $d\sigma/dt$ at four ISR energies. At $\sqrt{s}$ = 23 GeV the data are consistent with one-pion exchange. The dashed lines shown at the other energies represent the t dependence at 199.3 GeV/c of the ρ exchange reaction $\pi^- p \to \pi^0 n$ [12]. The data are consistent with these distributions.

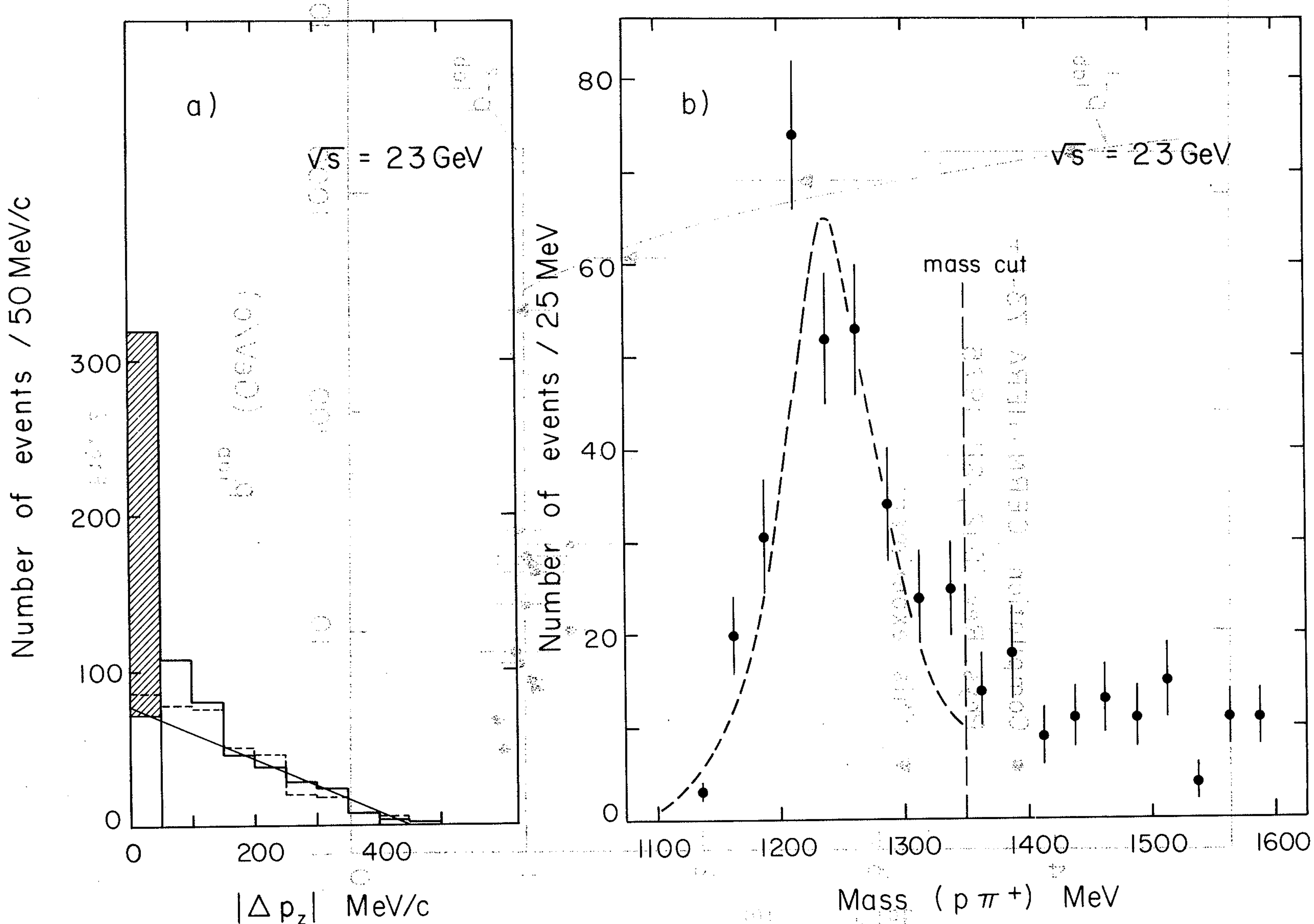

a)
√s = 23 GeV
Number of events / 50 MeV/c
0
100
200
300
0
200
400
|Δ p_z| MeV/c
b)
√s = 23 GeV
mass cut
Number of events / 25 MeV
0
20
40
60
80
1100
1200
1300
1400
1500
1600
Mass (p π+) MeV

Fig. 1

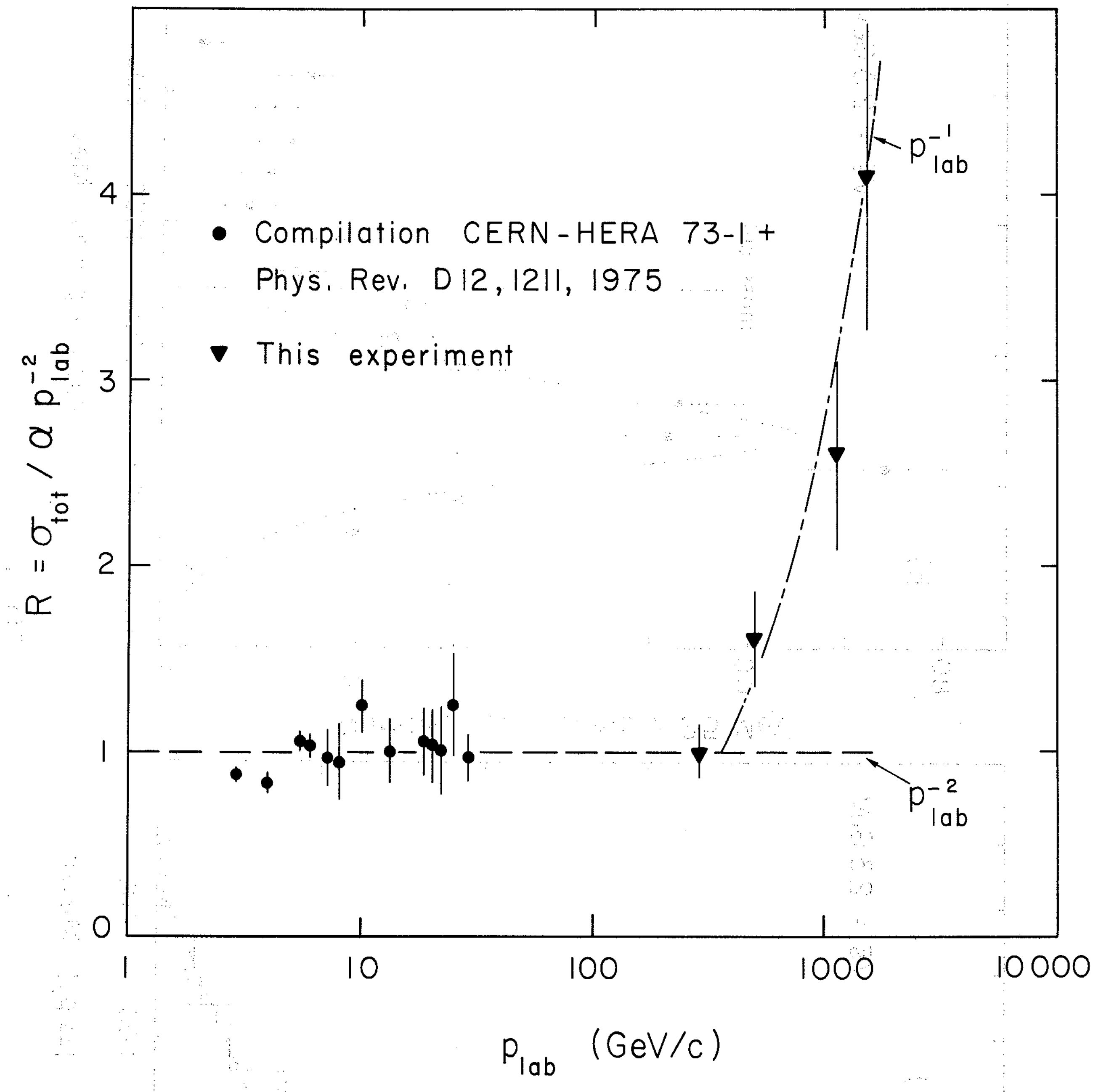

R = σ_{tot} / α p_{lab}^{-2}
0
1
2
3
4
1
10
100
1000
10 000
p_{lab} (GeV/c)
● Compilation CERN-HERA 73-1 +
Phys. Rev. D 12, 1211, 1975
▼ This experiment
p_{lab}^{-1}
p_{lab}^{-2}

Fig. 2

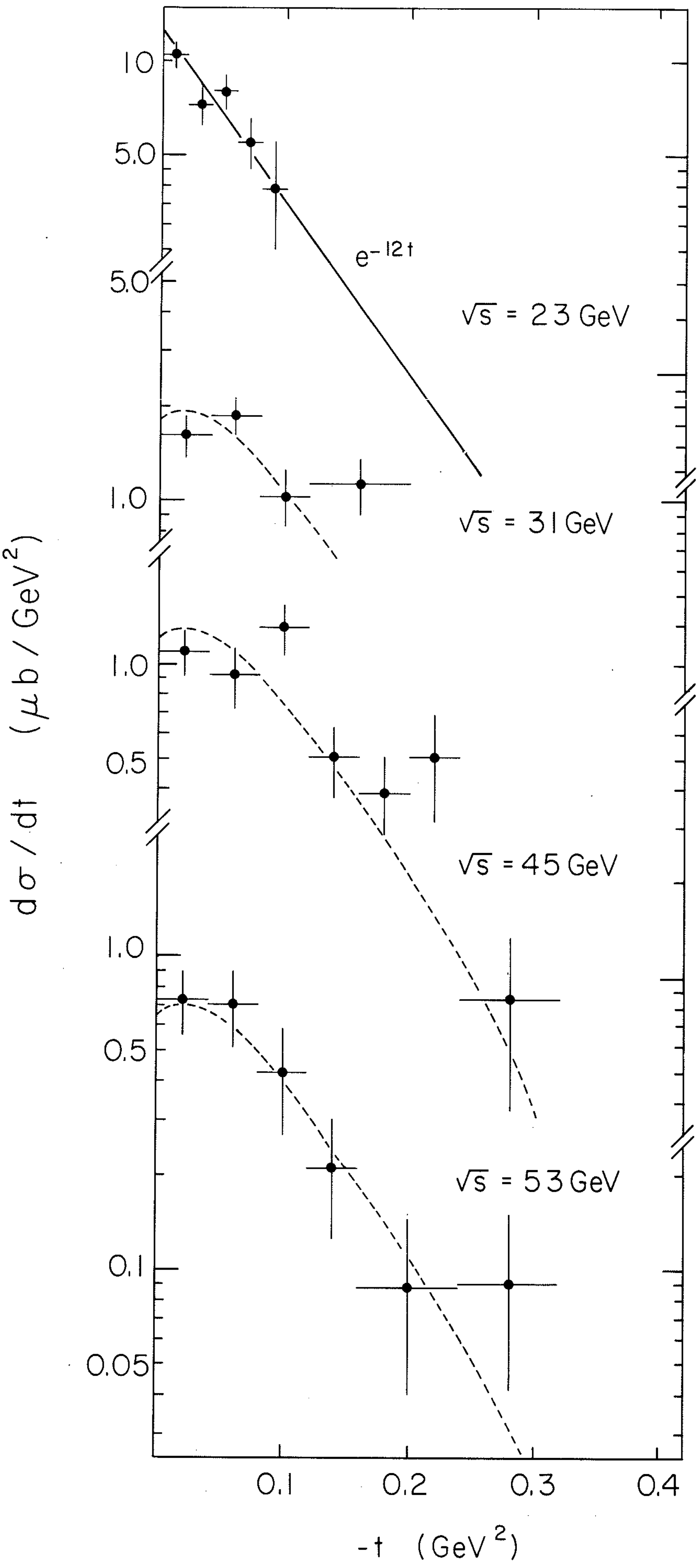

10
5.0
e^-12t
5.0
√s = 23 GeV
1.0
√s = 31 GeV
1.0
0.5
√s = 45 GeV
1.0
0.5
√s = 53 GeV
0.1
0.05
dσ / dt (μb / GeV²)
0.1
0.2
0.3
0.4
-t (GeV²)

Fig. 3